

# PHYSICAL REVIEW D

## PARTICLES AND FIELDS

THIRD SERIES, VOLUME 47, NUMBER 11

1 JUNE 1993

### RAPID COMMUNICATIONS

*Rapid Communications are intended for important new results which deserve accelerated publication, and are therefore given priority in editorial processing and production. A Rapid Communication in Physical Review D should be no longer than five printed pages and must be accompanied by an abstract. Page proofs are sent to authors, but because of the accelerated schedule, publication is generally not delayed for receipt of corrections unless requested by the author.*

#### Jets and jet multiplicities in high-energy photon-nucleon interactions

Loyal Durand and Katsuhiko Honjo

*Department of Physics, University of Wisconsin-Madison, Madison, Wisconsin 53706*

Raj Gandhi

*Department of Physics, Texas A&M University, College Station, Texas 77843*

Hong Pi

*Department of Theoretical Physics, University of Lund, Lund, Sweden S-22362*

Ina Sarcevic

*Department of Physics, University of Arizona, Tucson, Arizona 85721*

(Received 22 December 1992)

We discuss the theory of jet events in high-energy photon-proton interactions using a model which gives a good description of the data available on total inelastic  $\gamma p$  cross sections up to  $\sqrt{s}=210$  GeV. We show how to calculate the jet cross sections and jet multiplicities and give predictions for these quantities for energies appropriate for experiments at the DESY  $ep$  collider HERA and for very-high-energy cosmic ray observations.

PACS number(s): 13.60.Hb, 12.40.Pp, 13.87.Ce

The hadronic structure of the photon and its interaction with hadrons are currently subjects of considerable interest. The ZEUS and H1 groups at the  $ep$  collider HERA have presented preliminary results [1] on the  $\gamma p$  photoproduction cross section at 210 GeV center-of-mass energy which show the rise with energy typical of other hadronic interactions. It was shown by Gandhi and Sarcevic [2] in a simple model that this rise can be used to discriminate between different sets of photon structure functions. The hadronic behavior of the photon at very high energies ( $\sim 10^8$  GeV photon energy) is also of interest for the theory of air showers triggered by cosmic ray photons [3].

We have developed an improved QCD-based model of the photon interaction with nucleons [4] which gives predictions for the total inelastic  $\gamma p$  cross section which agree well with the data from the DESY  $ep$  collider HERA. The model has the interesting feature that the information needed to calculate  $\sigma_{\text{inel}}^{\gamma p}$  is largely determined

by high-energy  $\pi N$  scattering. In this paper, we will use the model to discuss the total jet cross section  $\sigma_{\text{jet}}^{\gamma p}$  and the probabilities for multiple-jet events, and give our predictions for those quantities at HERA energies and the energies relevant for cosmic ray experiments.

We begin by sketching our model for inelastic  $\gamma p$  scattering. The theory is developed in detail in [4]. The incoming physical photon state  $|\gamma\rangle_{\text{phys}}$  can be expressed as a superposition of the bare photon and the set of virtual hadronic states  $|m\rangle$  which can be distinguished in the subsequent interaction, and appear with probabilities  $\mathcal{P}_m$ . Accordingly, the total inelastic  $\gamma p$  cross section is given in a semiclassical picture as

$$\sigma_{\text{inel}}^{\gamma p} = (1 - \mathcal{P}_{\text{had}})\sigma_{\text{dir}} + \sum_m' \mathcal{P}_m \sigma^{m p}, \quad (1)$$

$$\mathcal{P}_{\text{had}} = \sum_m \mathcal{P}_m \ll 1.$$

Included among the states  $|m\rangle$  are low-mass vector meson states such as the  $\rho$ ,  $\omega$ , and  $\phi$ , and complex nonresonant final states which can be described on the average in a quark-gluon basis.

Whether the photon appears as a virtual vector meson state or a high-mass nonresonant state depends on the relative transverse momentum  $2p_{\perp 0}$  of the quark and antiquark in the virtual transition  $\gamma \rightarrow q\bar{q}$  which initiates the hadronic interaction. We note that  $p_{\perp 0} \approx 1/r_{\perp}$ , where  $r_{\perp}$  is the average transverse separation of the virtual quarks during the lifetime of the  $q\bar{q}$  system. If  $r_{\perp}$  is greater than, or on the order of, the average transverse radius  $R_{\perp} \equiv 1/Q_0$  of a vector meson, QCD confinement effects will clearly set in, and the  $q\bar{q}$  system will most likely appear in a hadronic collision as a light vector meson. For  $r_{\perp} < R_{\perp}$  the  $q\bar{q}$  system will be smaller than a vector meson. In this picture, the virtual hadronic system behaves for  $p_{\perp 0} < Q_0$  like a vector meson, and for  $p_{\perp 0} > Q_0$ , like a system with a transverse area smaller than that of a vector meson by a factor  $(Q_0/p_{\perp 0})^2$ . Its interaction cross section will be reduced accordingly.

After eikonalizing the hadronic cross sections using an impact parameter representation to account for possible multiple parton scatterings in a single  $\gamma p$  collision, the total inelastic  $\gamma p$  cross section is given by [4] as

$$\begin{aligned} \sigma_{\text{inel}}^{\gamma p} &= \sigma_{\text{dir}} + \lambda \mathcal{P}_{\rho} \int d^2b (1 - e^{-2\text{Re}\chi^{\rho p}}) \\ &+ \sum_q e_q^2 \frac{\alpha_{\text{em}}}{\pi} \int_{Q_0^2} \frac{dp_{\perp 0}^2}{p_{\perp 0}^2} \int d^2b (1 - e^{-2\text{Re}\chi^{q\bar{q}p}}). \end{aligned} \quad (2)$$

$$\sigma_{\text{QCD}}^{\rho p} = \sum_{ij} \frac{1}{1 + \delta_{ij}} \int_0^1 dx_1 \int_0^1 dx_2 \int_{p_{\perp, \text{min}}^2} dp_{\perp}^2 f_i^p(x_1, p_{\perp}^2) f_j^p(x_2, p_{\perp}^2) \frac{d\hat{\sigma}_{ij}}{dp_{\perp}^2}. \quad (6)$$

Using the equivalence of the  $\rho$  and  $\pi$  states in the quark model, we can equate the parton distribution and density profile functions for the  $\rho$  meson to the corresponding functions for the pion and take  $f_i^{\rho} = f_i^{\pi}$  and  $\rho_{\rho}(b) = \rho_{\pi}(b)$  [7]. The parton distributions in the pion are known reasonably well [8]. The density profile functions  $\rho_{\rho}(b)$  and  $\rho_{\pi}(b)$  can be taken as the Fourier transforms of the electromagnetic form factors of the proton and the  $\pi$  meson. The density overlap function  $A^{\rho p} \approx A^{\pi p}$  is then given by [9]

$$A^{\rho p}(b) = \frac{1}{4\pi} \frac{\nu^2 \mu^2}{\mu^2 - \nu^2} \left\{ \nu b K_1(\nu b) - \frac{2\nu^2}{\mu^2 - \nu^2} [K_0(\nu b) - K_0(\mu b)] \right\}, \quad (7)$$

where  $K_n(x)$  is a hyperbolic Bessel function, and the ‘‘size’’ parameters of the pion and the proton are  $\mu^2 = 0.47 \text{ GeV}^2$  and  $\nu^2 = 0.71 \text{ GeV}^2$ , respectively. The former corresponds to a root-mean-square transverse radius for the pion or  $\rho$  meson  $R_{\perp} = 1/Q_0 \approx 2/\mu$  with  $Q_0 \approx 340 \text{ MeV}$ .

The eikonal function for the  $q\bar{q}p$  scattering terms in Eq. (2) can be expressed similarly as

$$2\text{Re}\chi^{q\bar{q}p} = A^{q\bar{q}p}(b, p_{\perp 0}) [\sigma_{\text{soft}}^{q\bar{q}p}(s, p_{\perp 0}) + \sigma_{\text{QCD}}^{q\bar{q}p}(s, p_{\perp 0})]. \quad (8)$$

We assume that  $\rho_{q\bar{q}}(b)$  has the same form as  $\rho_{\rho}(b)$  ex-

cept with the size parameter  $\mu = 2Q_0$  of the  $\rho$  meson replaced by  $2p_{\perp 0}$  [4]. With this replacement,  $A^{q\bar{q}p}(b, p_{\perp 0})$  and  $\rho_{q\bar{q}}(b, p_{\perp 0})$  are continuous with the corresponding functions for the  $\rho$  meson at  $p_{\perp 0} = Q_0$ , but describe a shrinking system for  $p_{\perp 0} > Q_0$ . Finally, the cross-sections  $\sigma_{\text{soft}}^{q\bar{q}p}(s, p_{\perp 0})$  and  $\sigma_{\text{QCD}}^{q\bar{q}p}(s, p_{\perp 0})$  were assumed to scale with the physical cross-sectional area of the  $q\bar{q}$  system so that

The real part of the eikonal function for the  $\rho p$  interaction can be written in the form [6]

$$\begin{aligned} \text{Re}\chi^{\rho p}(b, s) &= \text{Re}\chi_{\text{soft}}^{\rho p}(s) + \text{Re}\chi_{\text{QCD}}^{\rho p}(b, s) \\ &= \frac{1}{2} A^{\rho p}(b) [\sigma_{\text{soft}}^{\rho p}(s) + \sigma_{\text{QCD}}^{\rho p}(s)], \end{aligned} \quad (3)$$

where  $A^{\rho p}(b)$  is the density overlap function,

$$A^{\rho p}(b) = \int d^2b' \rho_{\rho}(b) \rho_p(|\mathbf{b} - \mathbf{b}'|), \quad \int d^2b A^{\rho p}(b) = 1, \quad (4)$$

and  $\sigma_{\text{soft}}^{\rho p}$  and  $\sigma_{\text{QCD}}^{\rho p}$  are the soft- and hard-scattering parts of the intrinsic cross section.  $\sigma_{\text{soft}}^{\rho p}$  was parametrized in [4] using a Regge-like form,

$$\sigma_{\text{soft}}^{\rho p} = \sigma_0 + \sigma_1 (s - m_p^2)^{-1/2} + \sigma_2 (s - m_p^2)^{-1}, \quad (5)$$

while  $\sigma_{\text{QCD}}^{\rho p}$  was identified with the inclusive parton-level cross section for  $\rho p$  scattering,

cept with the size parameter  $\mu = 2Q_0$  of the  $\rho$  meson replaced by  $2p_{\perp 0}$  [4]. With this replacement,  $A^{q\bar{q}p}(b, p_{\perp 0})$  and  $\rho_{q\bar{q}}(b, p_{\perp 0})$  are continuous with the corresponding functions for the  $\rho$  meson at  $p_{\perp 0} = Q_0$ , but describe a shrinking system for  $p_{\perp 0} > Q_0$ . Finally, the cross-sections  $\sigma_{\text{soft}}^{q\bar{q}p}(s, p_{\perp 0})$  and  $\sigma_{\text{QCD}}^{q\bar{q}p}(s, p_{\perp 0})$  were assumed to scale with the physical cross-sectional area of the  $q\bar{q}$  system so that

$$\begin{aligned} \sigma_{\text{soft}}^{q\bar{q}p}(s, p_{\perp 0}) + \sigma_{\text{QCD}}^{q\bar{q}p}(s, p_{\perp 0}) \\ = (Q_0^2/p_{\perp 0}^2) [\sigma_{\text{soft}}^{\rho p}(s) + \sigma_{\text{QCD}}^{\rho p}(s)]. \end{aligned} \quad (9)$$

This model guarantees that  $\sigma_{\text{soft}}$  and  $\sigma_{\text{QCD}}$  are continuous at  $p_{\perp 0} = Q_0$ , and that the soft contributions from the  $q\bar{q}$  states die out as  $1/p_{\perp 0}^2$  as expected for higher twist terms. It neglects contributions to the  $q\bar{q}p$  cross section from the “pointlike” structure of the photon at high  $p_{\perp}$ , but these are known to be very small at the momentum transfers of interest [10]. The approximations used are closely connected to those used in vector dominance models, which describe the excited hadronic states as vector mesons with  $Vp$  cross sections that fall as  $1/M_V^2$  [4, 7].

We have calculated the total inelastic  $\gamma p$  cross section using Eq. (2) and the assumptions above. The soft cross section in Eq. (5) was determined [4] using the low-energy  $\gamma p$  data [11]. The fits in [4] give the values  $\sigma_0 = 25.8$  mb,  $\sigma_1 = 14.0$  mb GeV, and  $\sigma_2 = 14.0$  mb GeV<sup>2</sup> for the parameters in Eq. (5). The calculation used the parton distributions of Owens [8] for the pion and those of Eichten *et al.* [12] for the proton. The value of the parameter  $p_{\perp, \text{min}}$  in Eq. (6) which determines the transverse momentum at which hard parton-level collisions come into play was taken from a similar fit to  $\pi^{\pm}p$  scattering [9],  $p_{\perp, \text{min}} = 1.45$  GeV. The predicted cross section agrees with the preliminary HERA data [1] and those at lower energies as shown by the top curve in Fig. 1(a). The calculated rise in  $\sigma_{\text{inel}}^{\gamma p}$  at higher energies arises from the hard-scattering contributions, and is a prediction of the model rather than a fit to the HERA data. It is therefore of interest to look for other tests of the model. The jet cross sections predicted by the model provide one such test.

The total jet cross section  $\sigma_{\text{jet}}^{\gamma p}(s, Q^2)$  is defined for a cutoff  $Q$  for the transverse momentum of the observed jets to be the part of the inelastic  $\gamma p$  cross section which includes events with at least one semihard parton-parton (or  $\gamma$ -parton) scattering with  $p_{\perp}^2 \geq Q^2$ , irrespective of any soft processes that may occur. To find an expression for the jet cross section  $\sigma_{\text{jet}}^{mp}$  in the interaction between the proton and the hadronic state  $|m\rangle$  of the photon, we use the fact that semiclassically  $\exp[-2 \text{Re}\chi_{\text{QCD}}(b, s, Q^2)]$  can be interpreted as the probability that there is *no* parton-parton scattering with

$$\begin{aligned} \sigma_{\text{had}}^{mp}(s) &= \int d^2b \left( 1 - e^{-2 \text{Re}\chi_{\text{QCD}}^{mp} - 2 \text{Re}\chi_{\text{soft}}^{mp}} \right) \\ &= \int d^2b \left( 1 - e^{-2 \text{Re}\chi_{\text{soft}}^{mp'}(b, s, Q^2)} \right) e^{-2 \text{Re}\chi_{\text{QCD}}^{mp}(b, s, Q^2)} + \int d^2b \left( 1 - e^{-2 \text{Re}\chi_{\text{QCD}}^{mp}(b, s, Q^2)} \right) \\ &= \sigma_{\text{no jet}}^{mp}(s, Q^2) + \sigma_{\text{jet}}^{mp}(s, Q^2). \end{aligned} \quad (10)$$

Here

$$\sigma_{\text{jet}}^{mp}(s, Q^2) = \int d^2b \left( 1 - e^{-2 \text{Re}\chi_{\text{QCD}}^{mp}(b, s, Q^2)} \right) \quad (11)$$

is the total cross section for events associated with  $|m\rangle$  which contain jets with  $p_{\perp} \geq Q$ . The factor  $\sigma_{\text{QCD}}^{mp}$  which appears in the eikonal function in Eq. (11) is now to be evaluated using the expression in Eq. (6) with  $p_{\perp, \text{min}}^2$  replaced by  $Q^2$ . The remaining “no jet” cross section

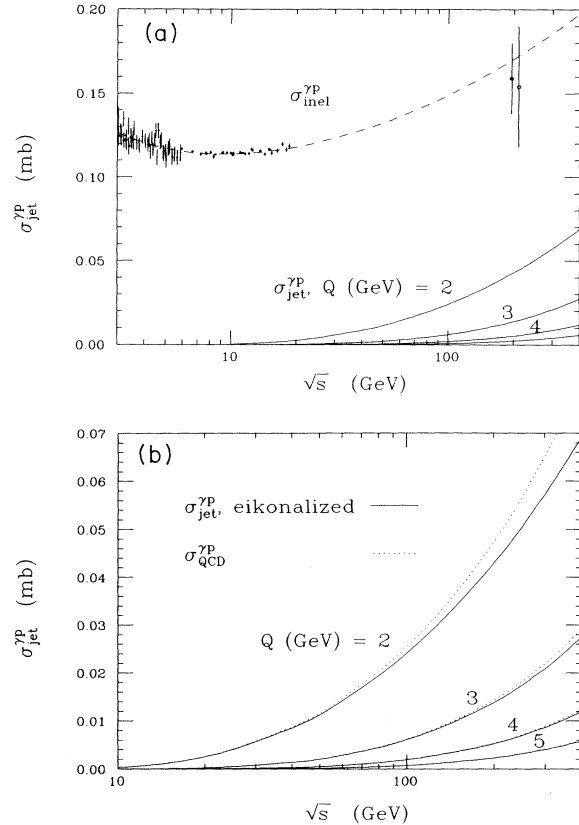


FIG. 1. (a) The calculated total jet cross sections as functions of  $\sqrt{s}$  and the transverse momentum cutoff  $Q$ . The total  $\gamma p$  inelastic cross section calculated in [4] is compared to the low-energy [11] and HERA [1] data in the upper curve. (b) The eikonized and inclusive jet cross sections for the same values of  $Q$ .

$p_{\perp}^2 \geq Q^2$  in a hadronic collision at impact parameter  $b$ . Using this observation, we can rewrite the expression for the total hadronic cross section  $\sigma^{mp}$  to separate the part which contains no jets with  $p_{\perp} \geq Q$  from a remaining jet cross section:

involves a modified eikonal function

$$\begin{aligned} \text{Re}\chi_{\text{soft}}^{mp'}(s, b, Q^2) &= \text{Re}\chi_{\text{soft}}^{mp} + \text{Re}\chi_{\text{QCD}}^{mp} \\ &\quad - \text{Re}\chi_{\text{QCD}}^{mp}(b, s, Q^2) \end{aligned} \quad (12)$$

which includes the usual soft term and additional contributions from jets softer than the (observational) cut imposed, that is, with  $p_{\perp, \text{min}} \leq p_{\perp} \leq Q$ .

The total jet cross section in  $\gamma p$  scattering is the gen-

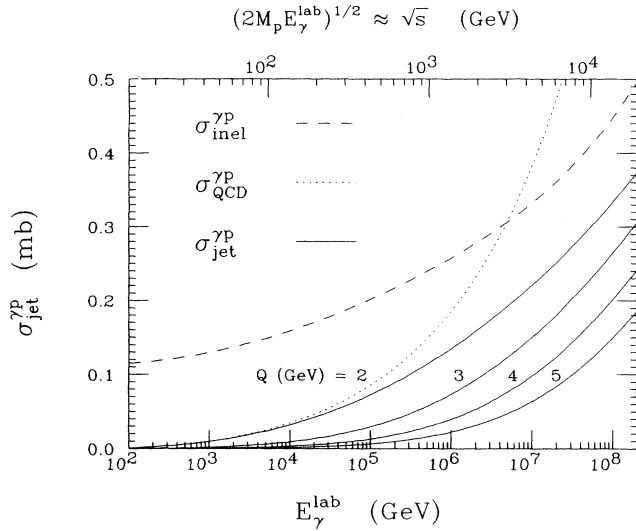


FIG. 2. The total inelastic and jet cross sections at cosmic ray energies.  $\sigma_{\text{QCD}}^{\gamma p}$  is the inclusive jet cross section.

eralized sum of the cross sections  $\sigma_{\text{jet}}^{mp}(s, Q^2)$ , weighted with the probabilities  $\mathcal{P}_m$ , over all the possible hadronic states of the photon, plus the very small jet contribution  $\sigma_{\text{dir}}(s, Q^2)$  from processes in which the photon interacts directly with a parton in the proton:

$$\begin{aligned} \sigma_{\text{jet}}^{\gamma p}(s, Q^2) &= \sigma_{\text{dir}}(s, Q^2) + \sum_m \mathcal{P}_m \sigma_{\text{jet}}^m \\ &= \sigma_{\text{dir}}(s, Q^2) + \lambda \mathcal{P}_\rho \sigma_{\text{jet}}^{\rho p}(s, Q^2) \\ &\quad + \sum_q e_q^2 \frac{\alpha_{\text{em}}}{\pi} \int_{Q_3^2} \frac{dp_{\perp 0}^2}{p_{\perp 0}^2} \sigma_{\text{jet}}^{q\bar{q}p}(s, Q^2, p_{\perp 0}^2), \end{aligned} \quad (13)$$

where

$$\sigma_{\text{dir}}(s, Q^2) = \sum_i \int_0^1 dx \int_{p_{\perp, \text{min}}^2} dp_{\perp}^2 f_i^p(x, p_{\perp}^2) \frac{d\hat{\sigma}_{\gamma i}}{dp_{\perp}^2}(s, p_{\perp}^2). \quad (14)$$

The jet cross sections for specific kinematic cuts, e.g., on jet angle, can be calculated using the same basic formulas with the cuts imposed on the integral for  $\sigma_{\text{QCD}}^{\rho p}$  in Eq. (6).

We have calculated the total jet cross section  $\sigma_{\text{jet}}^{\gamma p}$  in the HERA energy range for  $Q = 2, 3, 4,$  and  $5$  GeV, using the same parameters as were used in [4]. Our predictions are shown in Fig. 1(a) along with the calculated total inelastic  $\gamma p$  cross section and the experimental data [1, 11]. At  $\sqrt{s}=200$  GeV, the jet cross section is predicted to be approximately 1.3% of the total inelastic cross section for  $Q=5$  GeV in rough agreement with earlier predictions [2], and 25% of the total for  $Q=2$  GeV.

The rapid growth of the jet cross section with energy is associated with the growth of the parton distribution functions in the photon and the proton at the small values of  $x$  which become accessible at high energies. This

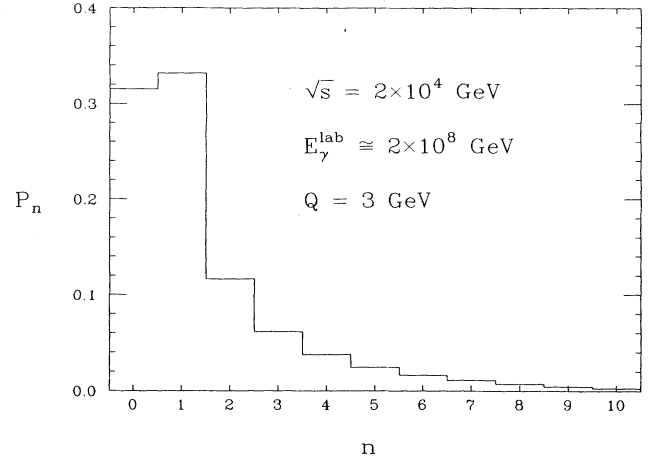


FIG. 3. The probability distributions for  $n$  parton-parton collisions or  $2n$  jets in a  $\gamma p$  collision.

growth also leads to an increasing probability of the scattering of more than one parton in a single  $\gamma p$  collision. For this reason, the inclusive parton-level  $\gamma p$  cross section  $\sigma_{\text{QCD}}^{\gamma p}$ , which counts each parton collision separately, is not the same as  $\sigma_{\text{jet}}^{\gamma p}$ . The latter has the overcounting due to multiple independent scatterings removed in the eikonalization. We show the effect of the eikonalization up to HERA energies in Fig. 1(b). The effect is not very significant for  $Q = 3, 4,$  and  $5$  GeV at  $\sqrt{s} = 200$  GeV, but causes about a 10% reduction in the jet cross section for  $Q = 2$  GeV.

In Fig. 2 we show  $\sigma_{\text{jet}}^{\gamma p}$  for the cosmic ray energy range for the same choices of  $Q$  as in Fig. 1, together with the calculated cross sections  $\sigma_{\text{inel}}^{\gamma p}$  and  $\sigma_{\text{QCD}}^{\gamma p}$  for  $Q = 2$  GeV. At very high energies, the jet cross section clearly comprises a large part of the total inelastic cross section, e.g., 75% of  $\sigma_{\text{inel}}^{\gamma p}$  at  $E_\gamma = 2 \times 10^8$  GeV ( $\sqrt{s} \approx 2 \times 10^4$  GeV) for  $Q = 2$  GeV. Even for  $Q = 5$  GeV,  $\sigma_{\text{jet}}^{\gamma p}$  gives nearly 40% of  $\sigma_{\text{inel}}^{\gamma p}$ . Also, as more of the incident partons scatter, the effect of eikonalization becomes quite large as shown for  $Q = 2$  GeV.

To calculate the multiplicity of jets, we note that the average number of parton-parton scatterings with  $p_{\perp} > Q$  in a single  $\gamma p$  collision at impact parameter  $b$  associated with the hadronic component  $|m\rangle$  of the pho-

TABLE I. Probabilities  $P_n$  of having  $n$  parton-parton collisions or  $2n$  jets in a single inelastic  $\gamma p$  collision at  $\sqrt{s}=200$  GeV.

$Q$ (GeV)	$P_0$	$P_1$	$P_2$	$P_3$
2	0.734	0.228	0.020	0.002
3	0.904	0.078	0.002	0.000
4	0.954	0.030	0.000	0.000
5	0.971	0.013	0.000	0.000

ton is

$$\bar{n}_m(b, s, Q^2) = \sigma_{\text{QCD}}^{mp}(s, Q^2) A^{mp}(b) = 2 \text{Re} \chi_{\text{QCD}}^{mp}(b, s, Q^2). \quad (15)$$

Since the parton-parton scatterings in our model are independent, the probability of having  $n$  scatterings ( $2n$

jets) in such a hadronic collision has a Poisson distribution

$$P_n^{mp}(b, s, Q^2) = \frac{1}{n!} [\bar{n}_m(b, s, Q^2)]^n e^{-\bar{n}_m(b, s, Q^2)}. \quad (16)$$

The probability  $P_n(s, Q^2)$  of having  $n$  scatterings relative to *all* the inelastic events at an impact parameter  $b$  is then

$$\begin{aligned} P_n(s, Q^2) &= (\sigma_{\text{inel}}^{\gamma p})^{-1} \sum_m \mathcal{P}_m \sigma_{\text{jet}, n}^{mp} \\ &= (\sigma_{\text{inel}}^{\gamma p})^{-1} \sum_m \mathcal{P}_m \int d^2b P_n^{mp}(b, s, Q^2) \\ &= (\sigma_{\text{inel}}^{\gamma p})^{-1} \sum_m \mathcal{P}_m \frac{1}{n!} \int d^2b [\bar{n}_m(b, s, Q^2)]^n e^{-\bar{n}_m(b, s, Q^2)} \end{aligned} \quad (17)$$

for  $n \geq 1$ .  $P_0(s, Q^2)$  is defined to be the probability of having a soft interaction with no associated jets:

$$P_0(s, Q^2) = (\sigma_{\text{inel}}^{\gamma p})^{-1} \sum_m \mathcal{P}_m \int d^2b \left(1 - e^{-2 \text{Re} \chi_{\text{soft}}^{mp}(b, s, Q^2)}\right) e^{-\bar{n}_m(b, s, Q^2)}. \quad (18)$$

Note that we have neglected the very small two-jet contribution to these expressions from the direct QCD interaction of the photon with the partons in the proton.

We have calculated  $P_n$  for  $n = 0, 1, 2$ , and 3 at  $\sqrt{s} = 200$  GeV using  $Q = 2, 3, 4$ , and 5 GeV. The results are shown in Table I. For  $Q = 5$  GeV the probability of having a 2-jet event (a single parton scattering) is about 1%; the probability for  $2n$ -jet events with  $n > 1$  is essentially zero. For  $Q = 2$  GeV the *total* probability of having any hadronic jet event is approximately 27%, with the 2-jet events comprising more than 90 % of the total.

We also investigated jet production in  $\gamma p$  scattering at very high energies. In Fig. 3 we show the distribution of  $P_n$  at  $\sqrt{s} = 2 \times 10^4$  GeV with the choice of  $Q = 3$  GeV. It is more likely at this energy to have jets in an event than

not, with an approximately 70% jet probability. While the 2-jet production is still the most probable, events with more than 2 jets occur with about 20% probability.

It will be quite interesting to see if the predictions above are verified in future experiments since they connect the hadronic properties of the photon directly to those of the pion. In particular, the jet structure of pion and photon-induced reactions on protons should be quite similar.

This work was supported in part through U.S. Department of Energy Grants Nos. DE-AC02-76ER00881 and DE-FG02-85ER40213. One of the authors (R.G.) would like to thank the World Laboratory for support.

- [1] The preliminary values of  $\sigma_{\text{inel}}^{\gamma p}$  are ZEUS Collaboration, Phys. Lett. B **293**, 465 (1992),  $\sigma_{\text{inel}}^{\gamma p} = 154 \pm 16 \pm 32 \mu\text{b}$  at an average energy of 210 GeV; H1 Collaboration, *ibid.* **299**, 374 (1993),  $\sigma_{\text{inel}}^{\gamma p} = 159 \pm 7 \pm 20 \mu\text{b}$  at 195 GeV.
- [2] R. Gandhi and I. Sarcevic, Phys. Rev. D **44**, R10 (1991).
- [3] See, for example, M. Drees and F. Halzen, Phys. Rev. Lett. **61**, 275 (1988); M. Drees, F. Halzen, and K. Hikasa, Phys. Rev. D **39**, 1310 (1989); T.K. Gaisser, F. Halzen, T. Stanev, and E. Zas, Phys. Lett. B **243**, 444 (1990).
- [4] K. Honjo, L. Durand, R. Gandhi, H. Pi, and I. Sarcevic, Phys. Rev. D (to be published).
- [5] There is evidence for considerable suppression of the cross section expected for photoproduction of the  $\phi$  relative to that for the  $\rho$  for  $\sqrt{s} \approx 10$  GeV. See R.M. Egloff *et al.*, Phys. Rev. Lett. **43**, 657 (1979). We therefore used  $\lambda = 10/9$  in the calculations reported here. This has rather little effect on the high-energy results [4].

- [6] L. Durand and H. Pi, Phys. Rev. Lett. **58**, 303 (1987); Phys. Rev. D **40**, 1436 (1989).
- [7] These assumptions are consistent with the near equality of measured  $\rho p$  and  $\pi p$  scattering cross sections, and with similar assumptions in the vector dominance model. See, for example, the review by T.H. Bauer, R.D. Spital, D.R. Yennie, and F.M. Pipkin, Rev. Mod. Phys. **50**, 261 (1978).
- [8] J.F. Owens, Phys. Rev. D **30**, 943 (1984).
- [9] L. Durand and H. Pi, Phys. Rev. D **43**, 2125 (1991).
- [10] J.R. Forshaw, Phys. Lett. B **285**, 354 (1992).
- [11] The lower energy data shown in Fig. 1 are from D.O. Caldwell *et al.*, Phys. Rev. Lett. **25**, 609 (1970); **40**, 1222 (1978).
- [12] E. Eichten, K. Lane, I. Hinchliffe, and C. Quigg, Rev. Mod. Phys. **56**, 579 (1984).